

Liquid film instability of wire coating

J-M. Buchlin and S. Zuccher

von Karman Institute, Rhode Saint Genèse, Belgium

Abstract

An experimental investigation of liquid film instability on a wire during free dip coating and annular jet wiping is presented. The experiments are conducted on a dedicated facility. The measurements are performed using laser sheet probes. The experimental observation leads to the characterisation of the instability in terms of wave speed, amplitude and amplification factor in function of the operating conditions.

1- Introduction

The coating of wires with a liquid film is encountered in many industrial processes. Different techniques such as free dip coating [1], annular jet wiping [2,] and die coating [3] are used.

The present study aims to provide fine experimental data concerning the features of the instability that develops during the two first wire coating processes quoted above. Emphasis is first placed on the experimental procedure including original non-intrusive optical measurement technique and data processing.

2- Experimental procedure

2.1 GALFIL facility

A close view of the GALFIN facility designed to study different wire coating techniques such as the dip-, die-coating and annular jet wiping is shown in figure 1. A complete description of the facility can be found in [2]. It is mainly composed of: a liquid bath (1), where the wire passes trough to be covered by a liquid layer; the metering device (2) that can be either a die or an annular-jet knife to control the final film thickness, two laser sheet probes (3) separated by a distance s which are described hereafter. During the experiments it was necessary to implement an ejector (4) because the wire covered by the liquid, touching the first pulley after the bath, produces a run-back flow that interferes with the coating. An evacuating tube (5) connects the ejector to a filter in order to recover the oil. Finally, a blade (6) cleans the wire after measurement of the final film thickness. The liquid used is silicon oil with density ranging from 900 to 970 kg/m³, viscosity from 0.01 to 0.5

Pa.s and surface tension of 0.02 Pa.m. The vertical position of the two probes (4) may be changed to perform measurements at different distances L from the liquid bath or from the jet nozzle. The wire tested has a radius r_0 equal to 1 mm.

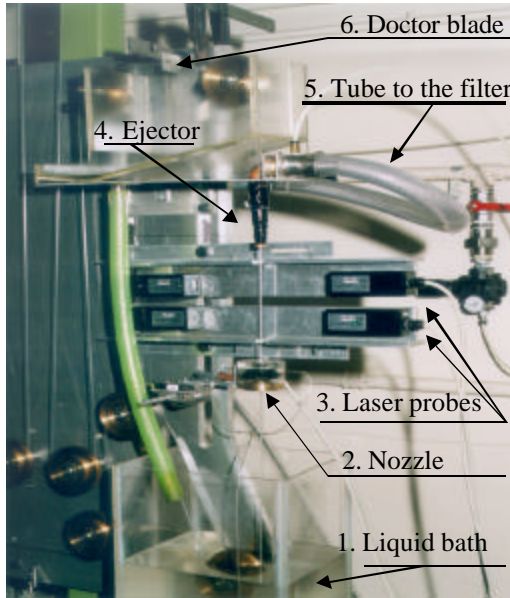


Figure 1: Views of the GALFIL facility

frequency of 3 kHz and a spatial resolution smaller than 5 mm. Two identical probes set at a certain known distance s allow the determination of the wave speed. The probes are connected to a PC implemented with a data acquisition card (figure 2).

The data processing includes several steps. The mean thickness of the liquid film h_0 is calculated from the time-dependent signal $h(t)$ yielded by the probes. The wave velocity c_0 is determined from the cross-correlation of the two signals. Once the wave velocity is obtained, the signal is transformed as a function of space Ox . The fast Fourier transform of the signal leads to the spectrum plotted in terms of wavelength ($\lambda = c_0/f$); a typical example is proposed in figure 3a. For each peak detected in the spectrum, the corresponding wavelength is isolated, its energy content is calculated and the signal

2.2 Measurement technique

To achieve good trade-off between high spatial resolution and sampling frequency to capture the free-surface wave in a wide range of wavelengths, a new optical probe is introduced. The principle relies on the obstruction by the wire of a narrow laser sheet of 1 mm thick and 5 mm wide produced by a collimated laser source as sketched in figure 2. An opto-electronic detector is placed in front of the laser source behind the wire. Calibration indicates that the output is linearly proportional (with a negative slope) to the diameter of the coated wire. Such a probe is characterised by a sampling

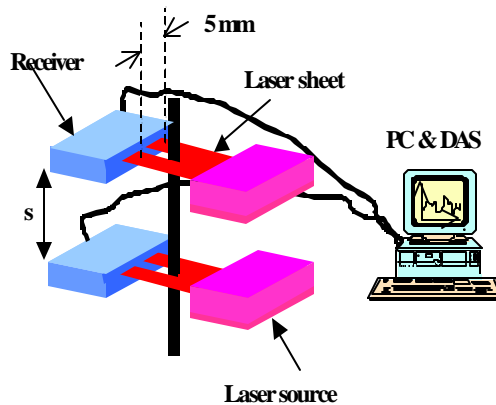


Figure 2: Measurement chain

is reconstructed to evaluate the monochromatic wave amplitude A_λ as illustrated in figure 3b.

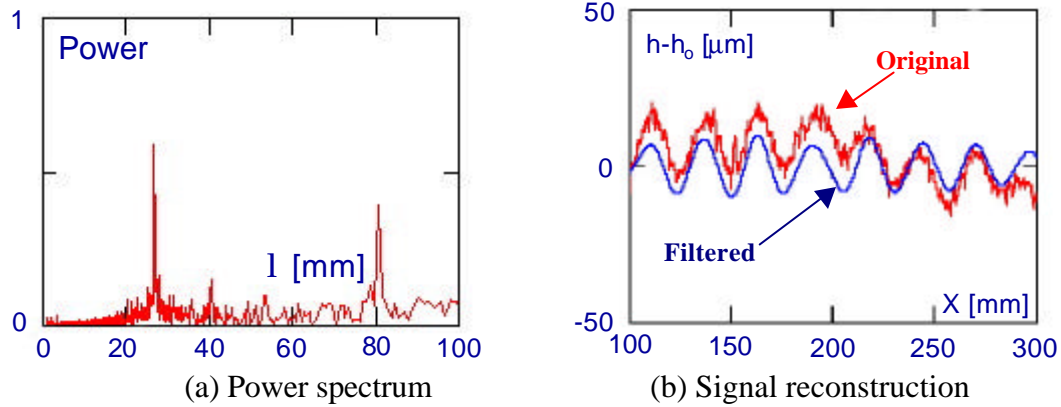


Figure 3: Typical steps of data processing

3 Typical results

3.1 Free dip coating

Figure 4 shows the evolution of the ensemble wave velocity expressed in terms of wave capillary number Ca_w versus the wire capillary number Ca for free dip coating experiments. The tests are performed changing the distance from the liquid bath L from 290 mm to 450 mm and the distance s between the two probes from 40 mm to 190 mm. Whatever the measurement conditions, the data are well reproduced indicating that the wave speed increases linearly with the wire velocity in good agreement with the theory developed by Lin & Liu [4] since the deviation does not exceed 10% as depicted in figure 4.

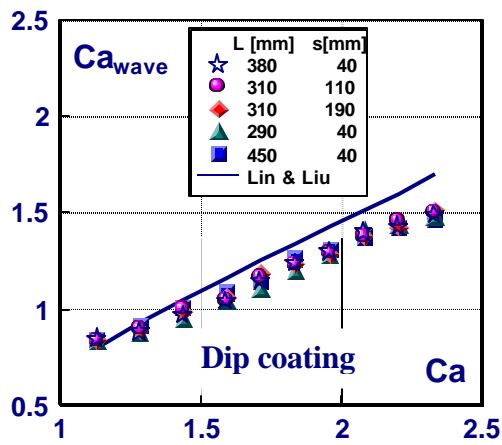


Figure 4: Capillary wave number

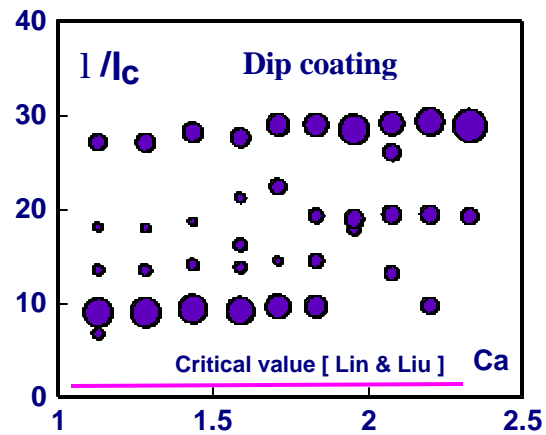


Figure 5: Wavelength content

The bubble chart in figure 5 presents the wavelength content of the liquid film instability. The wavelengths are normalised by the capillary length λ_c and the size of the bubble indicates the energy of each λ . The critical value λ_c predicted by the Lin & Liu theory [4] is also plotted in figure 5. It points out that the present dip coating flow exhibits an unstable character since the wavelengths are greater than

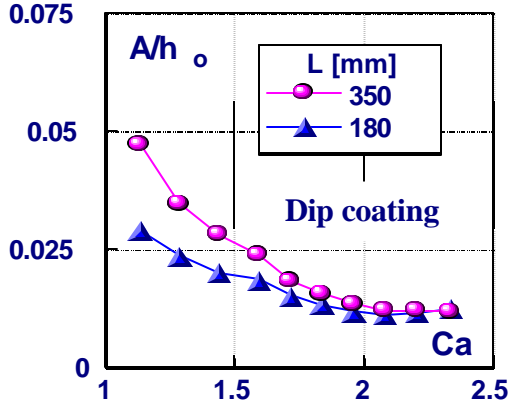


Figure 6: Wave amplitude

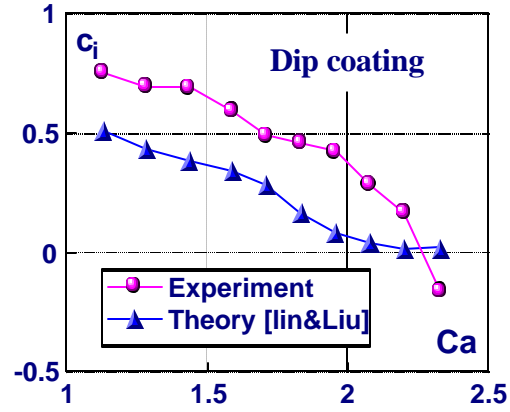


Figure 7: Amplification factor

λ_c . Figure 5 reveals a genuine behaviour featured by a transfer of energy content from small wavelengths (≈ 20 mm) at low capillary number (<1.8) to large wavelengths (≈ 55 mm) as Ca increases. Figure 6 compares the global amplitude of the instability reduced by the mean film thickness and measured at two distances L from the bath. It is worth noting that at low Ca -values the flow is unstable since the amplitude increases with L while it tends to become more stable as Ca increases. Such behaviour is clearly reflected by figure 7 that gives the plot of the

amplification factor defined as $c_i = \frac{c_o}{s} \ln\left(\frac{A_1}{A_2}\right)$. The experimental c_i -values are

higher than the value deduced from the small perturbation model introduced by Lin & Liu [4] probably due to non-linear effects. However, the trend that emphasises a drop of c_i as Ca augments is similar.

3.2 Annular jet wiping

Annular jet wiping tests show that the wave velocity does not depend on the measurement position L downstream the nozzle nor the operating air jet pressure ΔP_N as shown in figure 8. Again, Ca_w increases linearly with Ca . The experimental data are compared to a model developed at the VKI:

$$\frac{c_o}{V} = 1 - \text{Re} O^2 \left[\left[(2\Lambda^2 + 4\Lambda + 2) \ln\left(\frac{\Lambda + 1}{\Lambda}\right) - 2\Lambda - 1 \right] h + 1 \right]$$

Where V is the wire velocity and Λ is the typical curvature r_o/h_o . Re is the film Reynolds number based on the mean thickness and the free surface velocity while O is the Ohnesorge number $= \mathbf{m}/(rsh_o)^{1/2}$. η is a function of the pressure gradient $G=1+\nabla P/(\rho_ag)$ and the wall shear stress $S = \tau_j/(\rho_agh_o)$ generated by the air jet:

$$\eta = \frac{1}{2(\Lambda + 1)[G(\Lambda + 1) - 2S] \ln\left(\frac{\Lambda + 1}{\Lambda}\right) - G(2\Lambda + 1)}$$

Good agreement is observed at low capillary number where the non-linear effects are weaker.

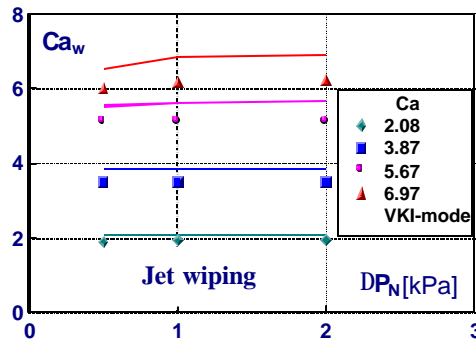


Figure 8: Effect of Ca on the wave speed

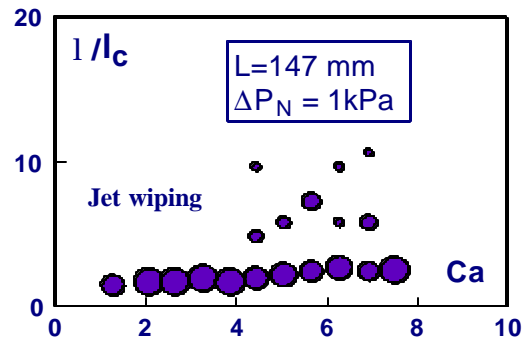


Figure 9: Wave length content

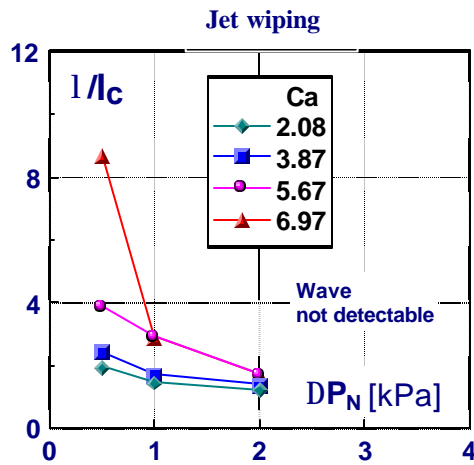


Figure 10: Effect of jet pressure on λ

In air-jet wiping the wavelength (≈ 4 mm) is smaller than in dip coating and does not evolve significantly with the wire capillary number. The energy content remains localised within the small λ (figure 9). Notice that the increase of the air jet pressure produces a thinning of the film thickness and a subsequent decrease of λ as depicted in figure 10. Above jet pressure of 2kPa, due to its limited resolution, the probe is not able to distinguish the wave amplitude from noise. Figures 11 and 12 emphasise the effect of the capillary number and air jet pressure, respectively, on the normalised amplitude and the amplification factor.

The increase of Ca provokes an increase of h_o faster than that of the wave amplitude. That explains why the negative value of the amplification factor increases indicating a stable coating. On the other hand, the augmentation of the air jet pressure has a propensity to make the resulting liquid film unstable; nevertheless, its parallel effect on the film thinning maintains the amplification negative. It is

worth noting that in annular jet wiping the initial relative amplitude exhibits rather large values, of the order of 40%. This implies that the phenomena are highly non-linear and that any small-perturbation theory is not appropriate.

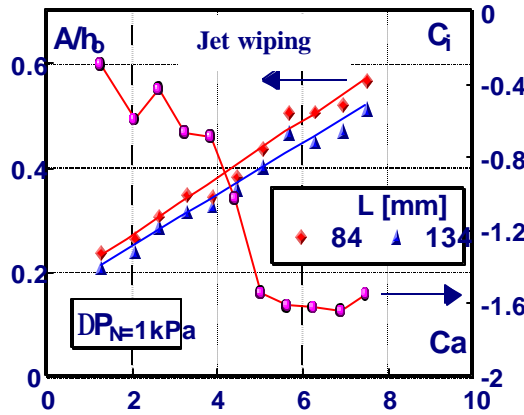


Figure 11: Ca -effect on the stability

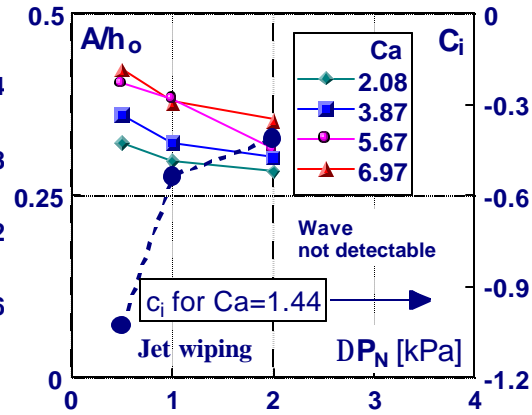


Figure 12: ΔP_N -effect of the stability

4- Conclusions

Liquid film instability during wire coating by free dipping process and annular jet wiping technique is investigated experimentally on a dedicated test facility implemented with original non-intrusive optical laser probes. A complete data processing allows the access to all the features of the instability. In the operating conditions considered, dip coating is generally unstable at $Ca < 2$ in agreement with the theory. Annular jet wiping yields stable liquid film as Ca increases but the augmentation of air jet pressure tends to rise the amplification factor.

5- References

1. Tallmadge, J.A. and Gutfinger, C. Entrainment of liquid films-drainage, withdrawal and removal, *Industral & Engineering Chemistry*, **59**, 19-34 (1967)
2. Parellada, C.; Anthoine, J. and Buchlin. J-M. Theoretical and experimental investigation of annular jet wiping, *Fluid Mechanics of Coating Processes-ECS-97 Proceeding*, Editor Bourgin. P, 204-211, Strasbourg (1997)
3. Buchlin, J-M; Arnalsteen, M. and Teuwissen, G. "Modelling of wire die coating" *Advances in Coating and Drying of Thin liquid Films-ECS-99*, Erlangen (1999).
4. Lin S. P., Liu W. C., *Instability of Film Coating of Wires and Tubes*, *AICHE J.*, **21**, No. 4, 775-782 (1975)